2. Nonlinear Wave Propagation

Strong laser pulses can induce a nonlinear polarization in matter. One example is a polarization that oscillates much slower than the incident light. This phenomenon can be employed in the generation of THz pulses. Similarly, a strong laser pulse temporally modifies the optical properties of a medium which are detected by a subsequent weak probe pulse. This effect can be used to scan the THz pulses or to study the dynamics of the optically excited medium in real time.

In this chapter, 2 classes of nonlinear polarization are discussed which are relevant for this work. By using a perturbational approach, we pay particular attention to the propagation of light when such nonlinear effects are present. These considerations are especially important to extract the dielectric function from the data of pump-probe experiments.

2.1. Wave Equation

Maxwell's equations yield a wave equation for the propagation of the *total* macroscopic electric field $\boldsymbol{E}(\boldsymbol{x}, t)$ in matter [Mil98],

$$\left(\boldsymbol{\nabla} \times \boldsymbol{\nabla} \times . + \frac{1}{c^2} \frac{\partial^2}{\partial t^2} \right) \boldsymbol{E} = -\frac{4\pi}{c^2} \frac{\partial^2}{\partial t^2} \boldsymbol{P},$$

where c is the vacuum speed of light, $\boldsymbol{x}$ and t points in space and time, respectively. The electric polarization $\boldsymbol{P}$ induced by $\boldsymbol{E}$ acts as a source term on the right-hand side of this equation and makes light propagation in matter different from that in vacuum where $\boldsymbol{P} = 0$.

In the following, we first restrict ourselves to a polarization linear in $\boldsymbol{E}$ which describes the domain of linear optics. Later, nonlinear contributions to $\boldsymbol{P}$ are taken into account and considered as small perturbations to calculate how they modify the propagation of the electric field.

2.2. Linear Optics

When we assume a medium in a steady state and consider only linear effects of $\boldsymbol{E}$ on $\boldsymbol{P}$, the induced polarization is given by Eq. (1.10). Switching from the time domain to frequency

space via a Fourier transformation results in the wave equation of linear optics

$$\left(\boldsymbol{\nabla} \times \boldsymbol{\nabla} \times . + \frac{\omega^2}{c^2}\varepsilon\right) \boldsymbol{E} = 0, \tag{2.1}$$

which is a linear and homogeneous differential equation.

If the medium is locally homogeneous and isotropic around $\boldsymbol{x}$, plane harmonic waves

$$\boldsymbol{E}(\boldsymbol{x}, t) = \boldsymbol{A} \exp(\mathrm{i}\boldsymbol{k}\boldsymbol{x} - \mathrm{i}\omega t)$$

with frequency $\omega/2\pi$, complex wavevector $\boldsymbol{k}$, and complex amplitude $\boldsymbol{A}$ are the eigenmodes of the electric field. Wavevector, frequency, and refractive index $n = \sqrt{\varepsilon}$ are connected by the so-called dispersion relation

$$c^2\boldsymbol{k}^2 = \omega^2 n^2.$$

The wavelength is given by $\lambda = 2\pi/|\mathrm{Re}\,\boldsymbol{k}|$, whereas $1/|\mathrm{Im}\,\boldsymbol{k}|$ is the attenuation length.

2.3. Nonlinear Polarization: 2 Examples

We now take the nonlinear part of the induced polarization into account, that is all deviations

$$\boldsymbol{P}_{\mathrm{NL}} := \boldsymbol{P} - \boldsymbol{P}^{(1)}$$

of $\boldsymbol{P}$ from the linear part $\boldsymbol{P}^{(1)}$. It appears as a source term on the right-hand side of the wave equation

$$\left(\boldsymbol{\nabla} \times \boldsymbol{\nabla} \times . + \frac{\omega^2}{c^2}\varepsilon\right) \boldsymbol{E} = 4\pi\frac{\omega^2}{c^2}\boldsymbol{P}_{\mathrm{NL}} \tag{2.2}$$

and thus perturbs the linear wave propagation.

$\boldsymbol{P}_{\mathrm{NL}}$ can, for instance, describe sum- and difference-frequency generation or the effect of the pump pulse on the propagation of the probe pulse in a pump-probe experiment. Before solving the wave equation, these examples of a nonlinear polarization are considered in more detail.

2.3.1. Sum- and Difference-Frequency Mixing: THz Generation and Detection

We consider only nonlinear effects to lowest order that is effects quadratic in $\boldsymbol{E}$. For a medium in a steady state one obtains [Gra78, Boy92]

$$P_i^{(2)}(\omega) = \sum_{jk} \int_{-\infty}^{\infty} \mathrm{d}\omega_1 \int_{-\infty}^{\infty} \mathrm{d}\omega_2 \; \chi_{ijk}^{(2)}(\omega, \omega_1, \omega_2) E_j(\omega_1) E_k(\omega_2)$$

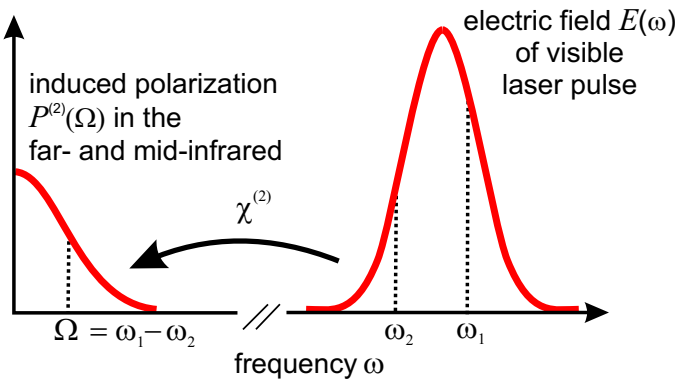

Figure 2.1.: Principle of THz generation. Each frequency pair (ω_1, ω_2) within the spectrum of a visible laser pulse generate a polarization at the difference frequency $\Omega = \omega_1 - \omega_2$.

with the abbreviation

$$\chi^{(2)}(\omega, \omega_1, \omega_2) = \chi^{(2)}(\omega_1, \omega_2)\, \delta(\omega - \omega_1 - \omega_2).$$

Here, $\chi^{(2)}(\omega_1, \omega_2)$ is the third-rank susceptibility tensor which vanishes in media with inversion symmetry. The δ-function shows that only the sum or difference of 2 light frequencies ω_1 and ω_2 can be generated by this 2nd-order process.

It is convenient to restrict oneself to positive frequencies $\omega, \omega_1, \omega_2 > 0$. By exploiting general symmetry properties of $\chi^{(2)}$, the 2nd-order polarization can be written as [Boy92]

$$P_i^{(2)}(\omega) = 2 \sum_{jk} \iint_{\omega_1 > \omega_2 > 0} \mathrm{d}\omega_1\, \mathrm{d}\omega_2 \tag{2.3}$$
$$\underbrace{\left[\chi_{ijk}^{(2)}(\omega, \omega_1, \omega_2) E_j(\omega_1) E_k(\omega_2)\right.}_{\text{sum-frequency components}} + \underbrace{\left.\chi_{ijk}^{(2)}(\omega, \omega_1, -\omega_2) E_j(\omega_1) E_k^*(\omega_2)\right]}_{\text{difference-frequency components}}$$

The 1st term in the integrand contributes for $\omega = \omega_1 + \omega_2$ and thus describes sum-frequency generation (SFG), whereas the 2nd term becomes operative for $\omega = \omega_1 - \omega_2$ and describes difference-frequency generation (DFG).

THz Generation

As visualized by Fig. 2.1, DFG can be employed to generate THz radiation of frequency $\Omega = \omega_1 - \omega_2$ from spectrally broad visible light of high intensity. For example, one of the lasers used in this work delivers pulses with a 100-nm bandwidth centered at 780 nm. Applying DFG to these pulses should result in THz pulses covering the spectrum from 0 to about 50 THz. In reality, however, propagation effects restrict the DFG process to those frequencies which fulfill the so-called "phase matching" condition. This point is discussed in Section 2.6.1.

It must be emphasized that the polarization induced by DFG does *not* depend on the absolute phase of all spectral components $E_j(\omega)$ since only the phase differences enter in Eq. (2.3).

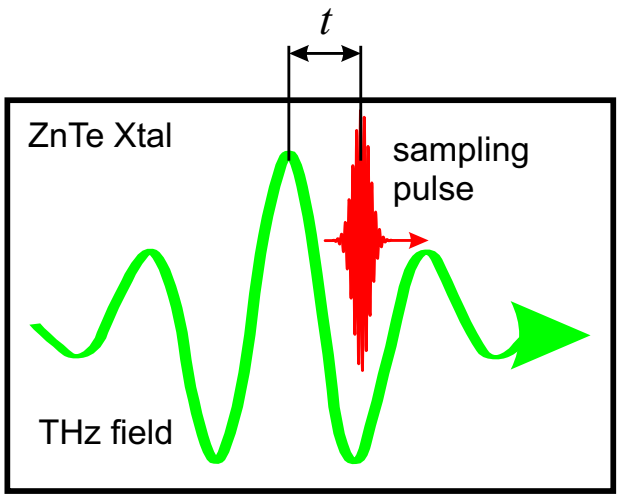

Figure 2.2.: Electrooptic detection of a THz waveform. The visible sampling pulse and the THz pulse propagate collinearly through the $\chi^{(2)}$ crystal. Due to the linear electrooptic effect, the visible pulse sees a birefringent medium where the birefringence is proportional to the THz electric field at the position of the sampling pulse. The resulting ellipticity of the sampling pulse is largest if both pulses propagate with the same velocity but vanishes if the sampling pulse sweeps over a complete THz cycle. To avoid this effect, ZnTe crystals of only 10 μm thickness are used [Lei99a].

THz Detection: Electrooptic Effect

DFG and SFG can be also employed to detect the THz radiation: When a visible laser pulse with field $\boldsymbol{E}_{\mathrm{VIS}}$ and a THz wave $\boldsymbol{E}_{\mathrm{THz}}$ travel collinearly through a crystal with $\chi^{(2)}_{ijk} \neq 0$, the THz wave effectively changes the refractive index for the visible pulse via the 2nd-order polarization (2.3). Due to this so-called electrooptic or Pockels effect the visible laser pulse "feels" the THz field which can be detected by this interaction.

More formally, the electrooptic effect can be reasoned as follows: The total field propagating through the crystal is $\boldsymbol{E} = \boldsymbol{E}_{\mathrm{THz}} + \boldsymbol{E}_{\mathrm{VIS}}$ and induces the nonlinear polarization (2.3). By retaining only cross terms, it has the formal structure $P^{(2)}_i \propto \sum_{jk} \chi^{(2)}_{ijk} E_{\mathrm{THz}j} E_{\mathrm{VIS}k}$ which just corresponds to an electric polarization linear in $\boldsymbol{E}_{\mathrm{VIS}}$. In other words, the contribution $\sum_j \chi^{(2)}_{ijk} E_{\mathrm{THz}j}$ represents a change in the linear optical properties of the medium due to the presence of the THz electric field.

The change in the linear susceptibility makes the crystal temporarily birefringent. In practice and as detailed in Fig. 2.2, this birefringence is measured by detecting the ellipticity the visible sampling pulse has accumulated due to its collinear propagation together with the THz pulse. As in many nonlinear processes, propagation effects limit the efficiency of the detection process.

2.3.2. Pump-Probe Experiments

The pump-probe technique is a method of choice to observe the dynamics of an optically excited sample with the best temporal resolution available. In such an experiment, a short pump pulse with a duration of typically 10 to 100 fs excites the sample, and the ensuing various relaxation processes can be studied by a temporally delayed probe pulse. After reflection from or transmission through the sample, the probe pulse pulse contains information about the current sample state, for instance, the temperature, magnetization, and so on.

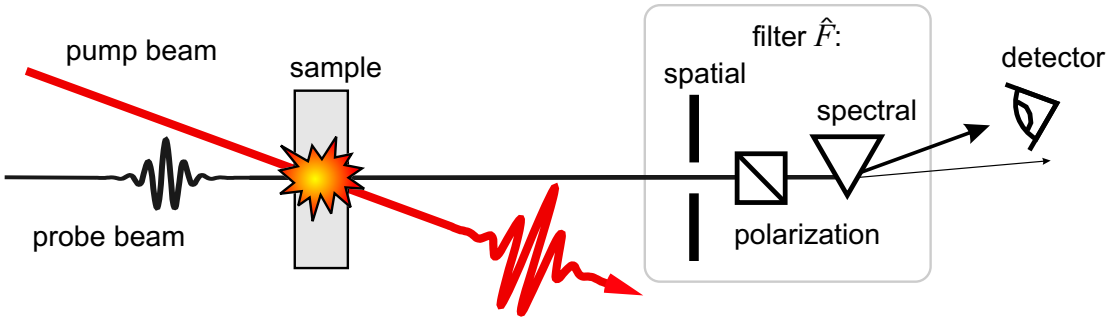

Figure 2.3.: Schematic of a pump-probe experiment. The sample is excited by an intense pump pulse and, after a delay τ, a weak probe pulse interacts with the sample and thereby gaining information about the current sample state. Before the probe pulse is detected, it passes some filtering scheme making sure that no pump light hits the detector when the probe beam is blocked. In this work, spectral and spatial filtering are employed.

From a formal point of view, the electric field $\boldsymbol{E} = \boldsymbol{E}_{\text{pump}} + \boldsymbol{E}_{\text{probe}}$ is incident on the sample in a pump-probe experiment and induces a nonlinear polarization $\boldsymbol{P}_{\text{NL}}$. Since often the probe field is weak, $|\boldsymbol{E}_{\text{probe}}| \ll |\boldsymbol{E}_{\text{pump}}|$, an expansion of $\boldsymbol{P}_{\text{NL}}[\boldsymbol{E}]$ with respect to $\boldsymbol{E}_{\text{probe}}$ is reasonable and similar to Eq. (1.29) yields

$$\boldsymbol{P}_{\text{NL}}(\boldsymbol{x}, t) = \boldsymbol{P}_{\text{NL}}[\boldsymbol{E}_{\text{pump}}] + \frac{1}{\sqrt{2\pi}} \int_{-\infty}^{\infty} \mathrm{d}t' \; \Delta\chi(\boldsymbol{x}, t, t') \boldsymbol{E}_{\text{probe}}(\boldsymbol{x}, t') + \mathcal{O}\left(\boldsymbol{E}_{\text{probe}}^2\right). \tag{2.4}$$

This approach takes also those nonlinear-polarization effects into account that cannot be described by a perturbation series like (1.9) any more, for example the field ionization of molecules.

The 1st term on the right-hand side of Eq. (2.4) describes a pump-induced polarization that would also occur without the probe pulse, for instance sum- and difference-frequency generation. The 2nd term contains all effects of the pump pulse and the sample on the weak probe pulse. Due to $\boldsymbol{P} = \boldsymbol{P}^{(1)} + \boldsymbol{P}_{\text{NL}}$, $\chi := \chi^{(1)} + \Delta\chi$ can be understood as the total linear polarization response of the system "*sample and pump pulse*", and

$$\Delta\varepsilon = 4\pi\Delta\chi$$

is the pump-induced change in the dielectric function of the sample.

THz detection can also be considered as a pump-probe experiment: As seen above, the THz pulse acts as the pump pulse and modifies the linear optical properties of a nonlinear medium which are seen by a copropagating visible probe pulse.

One conceptual problem remains: The separation $\boldsymbol{E} = \boldsymbol{E}_{\text{pump}} + \boldsymbol{E}_{\text{probe}}$ is well defined before the sample, but within the sample pump and probe beam interact with each other. Thus, the role of pump and probe beam is not clear any more after the sample. The most natural solution is to define the probe field as the field that is experimentally detected. It should disappear when the probe beam is blocked before the sample. Indeed, most experimental

setups apply spatial, spectral, or polarization filters to the total field $\boldsymbol{E}$ such that no light reaches the detector when the probe beam is blocked. When we formally represent this filter by a linear operator $\hat{F}$, the probe field is simply

$$\boldsymbol{E}_{\text{probe}} = \hat{F}\boldsymbol{E}.$$

It has a much smaller intensity than the "rest" $\boldsymbol{E}_{\text{pump}} = \boldsymbol{E} - \boldsymbol{E}_{\text{probe}}$. The considerations made above should be understood with these definitions of pump and probe beam.

The pump-probe configurations used in this work employ spectral filtering: In the THz *detection*, the pump and probe pulse are in the THz and visible spectral range, respectively. In TRTS, it is the other way around. We apply spectral filtering $\hat{F}_{\text{spec}}$ to Eq. (2.2) and obtain

$$\left(\boldsymbol{\nabla} \times \boldsymbol{\nabla} \times . + \frac{\omega^2}{c^2}\varepsilon\right) \boldsymbol{E}_{\text{probe}} = 4\pi \frac{\omega^2}{c^2} \hat{F}_{\text{spec}} \boldsymbol{P}_{\text{NL}},$$

since $\hat{F}_{\text{spec}}$ commutates with $\boldsymbol{\nabla}$ and ε. This equation together with (2.4) describes the probe field detected in a TRTS experiment. It is of the same structure as the general wave equation (2.2).

2.4. Solution of Wave Equation: Perturbational Approach

In this section, a method for the solution of the wave equation (2.2) is developed which is analog to the Born series in quantum scattering theory [Sch93]. As a perturbational method, it is only applicable when the nonlinear polarization does not affect the wave propagation too strongly. On the other hand, it gives an intuitive picture of the underlying mechanism and is easier to implement than numerical methods like the finite-difference time-domain scheme [Bea02]. In this work, it is applied to more complicated systems like carbon nanotubes embedded in a dielectric host where the pump beam induces additional anisotropies and inhomogeneities.

In order to find the solution of Eq. (2.2) we rewrite it as

$$\hat{D}\boldsymbol{E} = -\xi \cdot 4\pi \frac{\omega^2}{c^2} \boldsymbol{P}_{\text{NL}}$$

with the abbreviation

$$\hat{D} = \boldsymbol{\nabla}^2 - \boldsymbol{\nabla}(\boldsymbol{\nabla} \cdot .) - \frac{\omega^2}{c^2}\varepsilon$$

and consider its right-hand side as a perturbation. The perturbation parameter ξ will be set to $\xi = 1$ finally. The perturbation expansion of $\boldsymbol{E}$ with respect to ξ is

$$\boldsymbol{E} = \xi^0 \boldsymbol{E}^{(0)} + \xi^1 \boldsymbol{E}^{(1)} + \xi^2 \boldsymbol{E}^{(2)} + \dots . \tag{2.5}$$

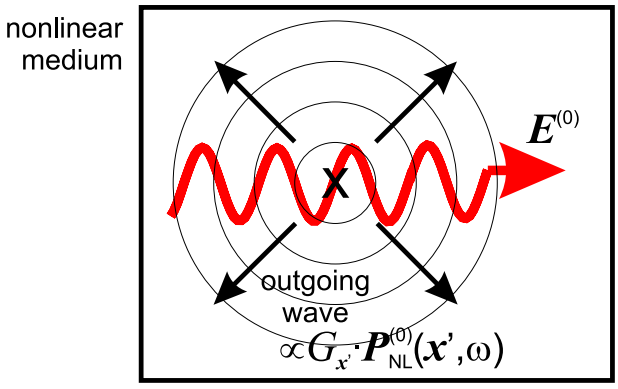

Figure 2.4.: The fundamental wave $\boldsymbol{E}^{(0)}$ travels through the medium according to linear optics. However, it induces a nonlinear polarization $\boldsymbol{P}_{\mathrm{NL}}^{(0)}$ at each position $\boldsymbol{x}'$ which in turn creates an outgoing wave $\propto \boldsymbol{P}_{\mathrm{NL}}^{(0)}(\boldsymbol{x}',\omega)\, G_{\boldsymbol{x}'}(\boldsymbol{x},\omega)$. All these waves add up to the 1st-order correction $\boldsymbol{E}^{(1)}$.

Its substitution in $\boldsymbol{P}_{\mathrm{NL}}(\boldsymbol{E})$, for example given by Eq. (2.3) or (2.4), yields an expansion of the nonlinear polarizability

$$\boldsymbol{P}_{\mathrm{NL}} = \xi^0 \boldsymbol{P}_{\mathrm{NL}}^{(0)} + \xi^1 \boldsymbol{P}_{\mathrm{NL}}^{(1)} + \xi^2 \boldsymbol{P}_{\mathrm{NL}}^{(2)} + \ldots,$$

where each coefficient $\boldsymbol{P}_{\mathrm{NL}}^{(j)}$ is a function of $\boldsymbol{E}^{(0)}, \ldots, \boldsymbol{E}^{(j)}$. Substitution in Eq. (2.2) leads to the following hierarchy of coupled differential equations:

$$\hat{D}\boldsymbol{E}^{(0)} = 0 \tag{2.6}$$

$$\hat{D}\boldsymbol{E}^{(1)} = -4\pi\frac{\omega^2}{c^2}\boldsymbol{P}_{\mathrm{NL}}^{(0)} \tag{2.7}$$

$$\vdots$$

$$\hat{D}\boldsymbol{E}^{(j+1)} = -4\pi\frac{\omega^2}{c^2}\boldsymbol{P}_{\mathrm{NL}}^{(j)} \tag{2.8}$$

$$\vdots$$

The 1st equation describes the wave propagation when all nonlinearities are switched off which is the domain of linear optics. The resulting "fundamental wave" $\boldsymbol{E}^{(0)}$ induces the lowest-order nonlinear polarization $\boldsymbol{P}_{\mathrm{NL}}^{(0)}$ which acts as a source for the 1st-order correction $\boldsymbol{E}^{(1)}$. Here, the term "source" becomes clear when the Green function $G_{\boldsymbol{x}'}(\boldsymbol{x},\omega)$ is employed to solve Eq. (2.8) for

$$\boldsymbol{E}^{(j+1)}(\boldsymbol{x},\omega) = -4\pi\frac{\omega^2}{c^2}\int \mathrm{d}^3\boldsymbol{x}'\, G_{\boldsymbol{x}'}(\boldsymbol{x},\omega)\, \boldsymbol{P}_{\mathrm{NL}}^{(j)}(\boldsymbol{x}',\omega). \tag{2.9}$$

The Green function is defined by the relation $\hat{D}G_{\boldsymbol{x}'} = \delta_{\boldsymbol{x}'}\mathbf{1}$ and can be understood as the wave that is scattered by a point-like spatial perturbation at $\boldsymbol{x}'$. It has to be an outgoing wave in order to fulfill the causality principle. For example, in case the unperturbed medium is spatially homogeneous and isotropic, $G_{\boldsymbol{x}'}$ is an outgoing spherical harmonic wave starting at $\boldsymbol{x}'$ [Jac83].

This result permits a simple interpretation of the perturbational solution: The wave $\boldsymbol{E}^{(0)} + \cdots + \boldsymbol{E}^{(j)}$ induces a polarization $\boldsymbol{P}_{\mathrm{NL}}^{(j)}$ which in turn at each point $\boldsymbol{x}'$ creates an outgoing wave

proportional to $\boldsymbol{P}_{\mathrm{NL}}^{(j)}(\boldsymbol{x}', \omega)$. All these outgoing waves add up to the next-order correction $\boldsymbol{E}^{(j+1)}$. Figure 2.4 illustrates the case $j = 0$ which in many cases already gives a good approximation.

2.5. 1-Dimensional Case

The solution (2.9) of the wave equation is still complicated since one has to integrate over 3-dimensional space with the Green-function being a 3×3 tensor. Fortunately, many cases of interest are effectively 1-dimensional: In all situations in this thesis, the light beams can be considered as plane waves which see a homogeneous medium across their beam cross section. Therefore, the problem can be reduced to the propagation along one axis z and a suitable component E of the electric field $\boldsymbol{E}$. Equation (2.8) becomes

$$\hat{D}E^{(j+1)}(z, \omega) = -4\pi \frac{\omega^2}{c^2} P_{\mathrm{NL}}^{(j)}(z, \omega) \tag{2.10}$$

with

$$\hat{D} = \partial_z^2 + k^2(z).$$

Here, $k(z)$ is the local wavevector of the fundamental wave given by

$$k^2 = \frac{\omega^2}{c^2} \varepsilon(z, \omega).$$

The derivation of Eq. (2.10) assumes $\boldsymbol{\nabla E} = 0$ and $P_{\mathrm{NL}}[\boldsymbol{E}] = P_{\mathrm{NL}}[E]$ which is fulfilled in all situations relevant for this work. The solution of Eq. (2.10) is analog to that of Eq. (2.9), but the 3-dimensional integration is reduced to an integration over z,

$$E^{(j+1)}(z, \omega) = -4\pi \frac{\omega^2}{c^2} \int \mathrm{d}z'\, G_{z'}(z, \omega)\, P_{\mathrm{NL}}^{(j)}(z', \omega). \tag{2.11}$$

2.5.1. Film between 2 Half-Spaces

A very frequent experimental configuration is shown in Fig. 2.5: A plane wave in the left-hand half-space (medium 1) is incident onto a film (medium 2) of thickness d, partially transmitted through the film into the right-hand half-space (medium 3), and partially reflected back. Multiple reflections at the 2 boundaries of the film lead to additional "echoes" propagating forward and backward.

Fundamental Wave

The fundamental wave $E^{(0)}$ in the 3 media 1, 2, and 3 is, respectively [Yeh88],

$$\frac{E^{(0)}}{E_{\mathrm{inc}}} = \begin{cases} \exp(-\mathrm{i}k_1 z) + A_1^- \exp(-\mathrm{i}k_1 z) & \text{(incident + reflected)} \\ A_2^+ \exp(\mathrm{i}k_2 z) + A_2^- \exp(-\mathrm{i}k_2 z) & \text{(forward + backward)} \\ A_3^+ \exp(\mathrm{i}k_3 z - \mathrm{i}k_3 d) & \text{(transmitted)} \end{cases} \tag{2.12}$$

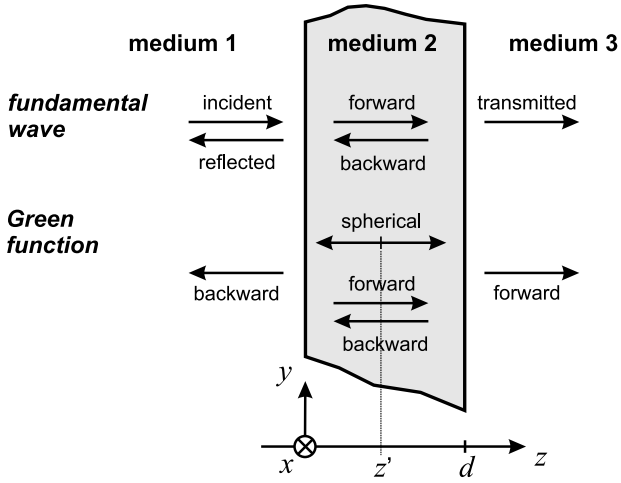

Figure 2.5.: Film of thickness d between 2 half-spaces. The fundamental wave is incident on the film from the left, partially reflected back and partially transmitted. The Green function has its source at $z = z'$ inside the film and creates an outgoing wave which also undergoes reflections at the 2 boundary planes of the film at $z = 0$ and $z = d$.

where E_{inc} is the incident electric field at $z = 0^-$ just before the left boundary. All coefficients are defined in Table 2.1. The quantities

$$t_{ij} = \frac{2n_i}{n_i + n_j} \quad \text{and} \quad r_{ij} = \frac{n_i - n_j}{n_i + n_j}$$

are the Fresnel transmission and reflection coefficients, respectively, for the case of normal incidence onto the boundary plane between medium i and j. The factor

$$M = \frac{1}{1 - r_{21} r_{23} \exp(2\mathrm{i}k_2 d)}$$

accounts for infinitely many reflections between the 2 boundary planes of the film which produce echoes in the reflected and transmitted beam. More generally, M can be expanded in a geometrical series

$$M = \sum_{j=0}^{\infty} \left[\exp(\mathrm{i}k_2 d)\, r_{23}\, \exp(\mathrm{i}k_2 d)\, r_{21}\right]^j$$

in which the jth term represents the jth reflection echo. The last expression nicely shows that the wave has to travel back and forth through the film between consecutive echoes. One can set $M = 1$ if multiple reflections are not important, for example in a thick film where the reflection echoes $j \geq 1$ are outside the temporal detection window.

Green Function

If the nonlinear response $\boldsymbol{P}_{\text{NL}}(z', \omega)$ is restricted to medium 2 with $z' \in [0, d]$, the Green function in medium 1, 2, and 3 becomes

$$2\mathrm{i}k_2 G_{z'}(z, \omega) = \begin{cases} B_1^- \exp(-\mathrm{i}k_1 z) & \text{(backward only)} \\ \exp(\mathrm{i}k_2 |z - z'|) + B_2^+ \exp(\mathrm{i}k_2 z) + B_2^- \exp(-\mathrm{i}k_2 z) & \text{(sph + fw + bw)} \\ B_3^+ \exp(\mathrm{i}k_3 z - \mathrm{i}k_3 d) & \text{(forward only)} \end{cases} \tag{2.13}$$

med	fundamental wave	Green function
1	$A_1^- = [r_{12} + r_{23}\exp(2\mathrm{i}k_2 d)]\,M$	$B_1^- = [\exp(\mathrm{i}k_2 z') + r_{23}\exp(2\mathrm{i}k_2 d - \mathrm{i}k_2 z')]\,t_{21} M$
2	$A_2^- = t_{12} r_{23}\exp(2\mathrm{i}k_2 d) M$	$B_2^- = B_3^+ \exp(\mathrm{i}k_2 d) r_{23}/t_{23}$
	$A_2^+ = t_{12} M$	$B_2^+ = B_1^- r_{21}/t_{21}$
3	$A_3^+ = t_{12} t_{23}\exp(\mathrm{i}k_2 d) M$	$B_3^+ = [\exp(-\mathrm{i}k_2 z') + r_{21}\exp(\mathrm{i}k_2 z')]\exp(\mathrm{i}k_2 d) t_{23} M$

Table 2.1.: Coefficients of the forward and backward propagating components of the fundamental wave $E^{(0)}$ and Green function $G_{z'}$ of a film between 2 half-spaces as described by Eqs. (2.12) and (2.13).

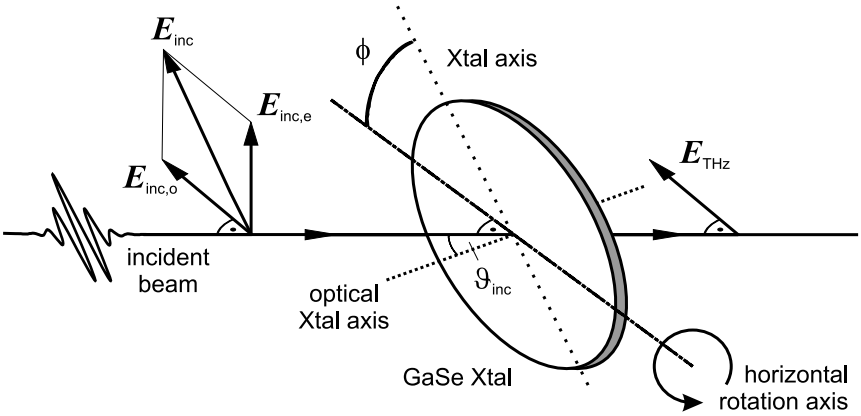

Figure 2.6.: Experimental geometry for THz generation in a GaSe crystal together with the definition of the angles ϕ and ϑ_{inc}.

respectively. This function fulfills $\hat{D}G_{z'} = \delta_{z'}$, is an outgoing wave, and, like its associated magnetic field, continuous at the film boundaries. The coefficients $B_j^{\pm}(z')$ depend on the center position z' of the Green function and are listed in Table 2.1.

2.6. Applications

2.6.1. THz Generation in GaSe

In this work, the optically uniaxial crystal GaSe is used to generate THz radiation from about 10 to 30 THz. The generation process is discussed in detail in Ref. [Sch05] based on the above formalism. Briefly, as shown in Fig. 2.6, the visible generation beam transmits a GaSe crystal where it propagates as an ordinary (o) and an extraordinary (e) wave with wavevectors $k_{\mathrm{o}}(\omega+\Omega)$ and $k_{\mathrm{e}}(\omega)$ and frequencies $\omega+\Omega$ and ω, respectively. Via difference-frequency mixing, both waves together create a polarization with frequency Ω along the ordinary direction if the azimuthal angle ϕ of the crystal is 60° [Sch05]. Application of the above formalism leads to a THz wave with wavevector $k_{\mathrm{o}}(\Omega)$ which is proportional to the so-called phase-matching factor

$$\frac{\exp(\mathrm{i}\Delta k d_{\mathrm{GaSe}}) - 1}{\Delta k} \quad \text{with} \quad \Delta k = k_{\mathrm{o}}(\omega+\Omega) - k_{\mathrm{e}}(\omega) - k_{\mathrm{o}}(\Omega)$$

at the output plane of the GaSe crystal [Kai99]. Therefore, an efficient THz generation of frequency Ω requires $|\Delta k d_{\mathrm{GaSe}}| \ll 1$. In order to fulfill this condition over a wide range of THz frequencies, GaSe crystals of a thickness d_{GaSe} of less than $100\,\mu$m are used [Hub00].

2.6.2. Probe-Pulse Propagation

Exciting the film in Fig. 2.5 by a pump pulse at time $t = -\tau$ leads to a change $\Delta\varepsilon_{t+\tau}(\omega)$ in the dielectric function of the film which is seen by the THz probe pulse E arriving at time $t = 0$ at the sample. Here, $\Delta\varepsilon_t$ means the instantaneous dielectric function as defined in Section 1.8.2. Since all experiments in this work are transmission experiments, we calculate the probe pulse $E(z = d + 0^+, \omega)$ directly after the film.

According to Eqs. (2.4) and (1.33), the relevant nonlinear polarization in ω space is

$$P_{\mathrm{NL}\tau}(z,\omega) = \int \mathrm{d}\omega'\, \Delta\varepsilon_{\omega-\omega'}(z,\omega') E(z,\omega')\, \mathrm{e}^{-\mathrm{i}(\omega-\omega')\tau}.$$

It induces a pump-induced change $\Delta E_\tau(d + 0^+, \omega)$ in the electric field directly after the film which can be calculated by the aid of Eq. (2.11). To 1st order in $\Delta\varepsilon$, one obtains

$$\Delta E_\tau(d+0^+,\omega) = -\frac{\omega^2}{c^2} \int \mathrm{d}z \int \mathrm{d}\omega'\, \Delta\varepsilon_{\omega-\omega'}(z,\omega')\, \mathrm{e}^{-\mathrm{i}(\omega-\omega')\tau} E^{(0)}(z,\omega') G_z(d+0^+,\omega).$$

In a pump-probe experiment, ΔE_τ is detected for a complete sequence of pump-probe delays τ. In order to get access to the dielectric function, we apply a Fourier transformation $\tau \longrightarrow \Omega$ to the last equation and find

$$\Delta E_\Omega(d+0^+,\omega) = -\frac{\omega^2}{c^2} \int \mathrm{d}z\, \Delta\varepsilon_\Omega(z,\omega-\Omega) E^{(0)}(z,\omega-\Omega) G_z(d+0^+,\omega).$$

Inserting the expressions (2.12) and (2.13) for the fundamental wave $E^{(0)}$ and the Green function $G_z(d + 0^+, \omega)$, respectively, leads to a quite lengthy relation between the incident field E_{inc} and the pump-induced change $\Delta E_\Omega(d + 0^+, \omega)$ in the transmitted field.

However, the films used in this work are much thinner than the wavelength of the THz probe radiation such that one can set $\exp(\mathrm{i}k_2 d) = 1$. As a consequence, the fundamental wave is $E^{(0)}(d + 0^+, \omega) = E_{\mathrm{inc}} t_{12} t_{23} M = R_\infty E_{\mathrm{inc}}$ where

$$R_\infty = \frac{E^{(0)}(d+0^+,\omega)}{E_{\mathrm{inc}}} = \frac{t_{12}t_{23}}{1 + r_{12}r_{23}} \tag{2.14}$$

is the response of the unexcited sample. The Green function (2.13) can be written as $G_z(d + 0^+, \omega) = B_3^+/2\mathrm{i}k_2 = R_\infty/2\mathrm{i}k_1$ which leads to the compact relation

$$\Delta E_\Omega(d+0^+,\omega) = \Delta R_\Omega(\omega-\Omega) E_{\mathrm{inc}}(\omega-\Omega). \tag{2.15}$$

Here, the pump-induced change

$$\Delta R_\Omega(\omega-\Omega) = \frac{\mathrm{i}\omega}{2cn_1(\omega)} R_\infty(\omega-\Omega) R_\infty(\omega) \int \mathrm{d}z\, \Delta\varepsilon_\Omega(z,\omega-\Omega) \tag{2.16}$$

in the sample response function is the experimentally accessible quantity and can be easily solved for the spatially averaged change in the dielectric function. In the course of this work, this formula will be applied to thin films of graphite and carbon nanotubes.

If all terms with the argument $\omega-\Omega$ in Eq. (2.15) are sufficiently flat, this argument can be approximated by $\omega-\Omega\approx\omega$. An inverse Fourier transformation with respect to Ω yields

$$\Delta R_\tau(\omega) = \frac{\Delta E_\tau(d+0^+,\omega)}{E_\mathrm{inc}(\omega)} = \frac{\mathrm{i}\omega}{2cn_1} R_\infty(\omega)^2 \int \mathrm{d}z\, \Delta\varepsilon_\tau(z,\omega), \tag{2.17}$$

which can be interpreted as the quasistatic limit of Eq. (2.15): The wave propagates as if the sample changes its optical properties only very slowly.

WKB Approximation

We assume a quasistatically changing sample such that the wave equation (2.10) can be rewritten as

$$\left[\partial_z^2 + k_\tau^2(z)\right] E_\tau(z,\omega) = 0 \tag{2.18}$$

with

$$k_\tau^2 = \frac{\omega^2}{c^2}[\varepsilon_\infty(z,\omega) + \Delta\varepsilon_\tau(z,\omega)].$$

When a wave is incident from $z=-\infty$ and equals E_inc at $z=z_0$, the field at a position $z>z_0$ is, according to the so-called WKB approximation, given by [Sch93]

$$E_\tau(z,\omega) = E_\mathrm{inc} \exp\left[\mathrm{i}\int_{z_0}^{z} \mathrm{d}z'\, k_\tau(z')\right]. \tag{2.19}$$

The WKB approximation is valid if the local wavevector k_τ varies only slightly over 1 wavelength of the radiation, that is, if $|\partial k_\tau/\partial z| \ll |k_\tau^2|$ [Sch93].